Vibrational and Quantum Chemical investigation of cyclization of thiosemicarbazide group in 1-benzoyl-4-phenyl-3- thiosemicarbazide

Priyanka Gautam, Om Prakash, R.K. Dani, N.K. Singh, Ranjan K. Singh

PII: S1386-1425(14)00506-X
DOI: http://dx.doi.org/10.1016/j.saa.2014.03.095
Reference: SAA 11928

To appear in: *Spectrochimica Acta Part A: Molecular and Biomolecular Spectroscopy*

Received Date: 25 October 2013
Revised Date: 28 February 2014
Accepted Date: 18 March 2014

Please cite this article as: P. Gautam, O. Prakash, R.K. Dani, N.K. Singh, R.K. Singh, Vibrational and Quantum Chemical investigation of cyclization of thiosemicarbazide group in 1-benzoyl-4-phenyl-3- thiosemicarbazide, *Spectrochimica Acta Part A: Molecular and Biomolecular Spectroscopy* (2014), doi: http://dx.doi.org/10.1016/j.saa.2014.03.095

Vibrational and Quantum Chemical investigation of cyclization of thiosemicarbazide group in 1-benzoyl-4-phenyl-3- thiosemicarbazide

Priyanka Gautam[a], Om Prakash[a], R.K. Dani[b], N.K. Singh[b], Ranjan K. Singh[a]*

[a]Department of Physics, Banaras Hindu University, Varanasi- 221005, India.
[b]Department of Chemistry, Banaras Hindu University, Varanasi- 221005, India

Abstract

1-benzoyl-4-phenyl-3-thiosemicarbazide (H_3bpt) was treated with acid - base in one sequence and base – acid in other sequence, both of which lead to ring formation of thiosemicarbazide group, giving N-phenyl-5-phenyl-1,3,4-thiadiazol-2-amine (Hppta) in the first case and 4,5-diphenyl-2,4-dihydro-1,2,4-triazole-3-thione (Hdptt) in the second case. The primary (H_3bpt) as well as the resulting compounds (Hppta & Hdptt) has been characterized by elemental analyses, NMR, FTIR and Raman spectroscopic techniques. The quantum chemical calculations of the compounds are performed using DFT/B3LYP/6311G(d,p) method for geometry optimizations and also for prediction of the molecular properties. The cyclization is confirmed by disappearance of many bands belonging to the open chain subgroups of H_3bpt such as; N-H stretching, N-H bending, C-N stretching, N-H puckering, C=O stretching etc. The ring formation of 1-benzoyl-4-phenyl-3-thiosemicarbazide (H_3bpt) has been further confirmed by the appearance of many bands belonging to the closed ring of thiosemicarbazide in the resulting compounds Hppta and Hdptt.

Keywords: Thiosemicarbazide, Thiadiazole, Triazole, FT-IR, Raman and DFT.

*Correpsondence author e-mail: *ranjanksingh65@rediffmail.com*

1. Introduction:

Heterocyclic aromatic compounds contained N, S and O in the ring are biologically active and pharmaceutically important [1-5]. The derivatives of triazole and thiadiazole have been found to possess a wide spectrum of pharmacological, medical and biological activities [6-9]. The derivatives of triazole and thiadiazole could be synthesized from the derivatives of 1-benzoyl-3-thiosemicarbazide followed by ring formation of thiosemicarbazide group by treating with acid followed by base or base followed by acid [10-12]. The thiosemicarbazides being building blocks for the synthesis of a variety of heterocyclic ring compounds is useful to design therapeutically useful drugs. The ring formation and opening mechanisms are important and crucial because a drug in open or closed chain form affects biologically induced reaction and metabolic process differently. The cyclization/ decyclization phenomena in vivo is generally induced by catalyst. However, it can be induced by varying temperature/ pH of the medium [13-15]. The FTIR and Raman spectroscopy combined with quantum chemical computation may give fingerprint of this process.

The main purpose of this work is to investigate the ring formation phenomenon of thiosemicarbazide group of the 1-benzoyl-4-phenyl-3-thiosemicarbazide, resulting the molecules N-phenyl-5-phenyl-1,3,4-thiadiazole-2-amine and 4,5-diphenyl-2,4-dihydro-1,2,4-triazole-3-thione, by the means of combined FTIR, Raman and DFT technique and elucidate the structural information with molecular properties. The quantum chemical calculation of the compounds are performed using DFT/B3LYP/6311G(d,p) method [16-18] for geometry optimizations and also for prediction of the molecular properties viz. charge distribution, molecular electrostatic potentials surfaces, frontier molecular orbital and reactive sites for electrophilic attack and neucleophilic reaction. The vibrational assignments

of the IR and Raman bands are carried out by using GAR2PED software [19]. We also made the comparisons between experimental results with computed one.

2. Experimental:

2.1 Materials: Methyl benzoate, Phenyl isothiocyanate (Sigma Aldrich), Conc. H_2SO_4 (SD Fine Chemicals) and NaOH, hydrazine hydrate (Qualigens) were used. The reagents were used without further purification and all experiments. All the synthetic manipulations were carried out in open atmosphere and at room temperature. The solvents were dried and distilled before use following the standard procedure.

2.2 Synthesis:

2.2.1: 1-benzoyl-4-phenyl-3-thiosemicarbazide (H_3bpt): A mixture of benzoic acid hydrazide (2.160 g, 20 mmol) and phenyl isothiocyanate (2.4 mL, 20 mmol) in benzene was refluxed for 8 h at 80 ºC, from which white precipitate of 1-benzoyl-4-phenyl-3-thiosemicarbazide was obtained after cooling. The precipitate was filtered off, washed with water and diethyl ether, air dried and crystallized from ethanol.

2.2.2: N-phenyl-5-phenyl-1,3,4-thiadiazole-2-amine (Hppta): 1-benzoyl-4-phenyl-3-thiosemicarbazide (2.813 g, 10 mmol) was added slowly in 10 ml conc. H_2SO_4 and stirred for 2 h at low temperature. The mixture was poured over crushed ice and the precipitated solid was filtered off, washed twice with cold water and dried. The yellow compounds were obtained by slow evaporation of solvent for 15 days.

2.2.3: 4,5-diphenyl-2,4-dihydro-1,2,4-triazole-3-thione (Hdptt): A stirring mixture of 1-benzoyl-4-phenyl-3-thiosemicarbazide (2.813 g, 10 mmol) and NaOH (0.4 g, 10 mmol) in ethanol 25 mL was refluxed for 6 h at 65 ºC. After cooling, the solution was acidified with dil. HCl (6 mL, 30%, v/v) and the precipitate of 4,5-diphenyl-2,4-dihydro-1,2,4-triazole-3-thione was filtered off and crystallized from ethanol.

The synthesis of compounds H_3bpt, Hppta and Hdptt are depicted in scheme 1 (in supplementary part).

2.3. Instrumentation and measurements: Carbon, hydrogen and nitrogen contents were estimated on an Elementar Vario EL III Carlo Erbo 1108. FT-IR spectra were recorded in the 4000–400 cm^{-1} region in KBr pellets on Spectrum 65 FT-IR spectrometer from PerkinElmer. ^{1}H and ^{13}C NMR spectra were recorded in DMSO-d_6 on a JEOL AL300 FT NMR spectrometer using TMS as an internal reference. Initially benzoic acid hydrazide was prepared by refluxing equimolar amount of methyl benzoate and hydrazine hydrate at 75 ºC for 5h.

The laser Raman spectra were recorded on a Raman spectrometer from Renishaw Model: RM 1000 having grating of 2400 grooves/mm giving spectral resolution of ~1 cm^{-1} at 50 micron slit opening. The 514.5 nm Ar^{+} -laser was used as an excitation source delivering ~5 mW intensity at the sample. A microscope from Olympus with 50 x objectives was used to focus the laser on the sample and to collect the Raman scattered signal in back scattering geometry. The Raman spectra were recorded in the range 200-3500 cm^{-1}. Spectrometer scanning, data collection and processing were done by a dedicated computer using Gram Wire software.

3. Computational details:

All quantum chemical calculations and the geometry optimization of compounds H_3bpt, Hppta and Hdptt have been performed with Gaussian 03 and GaussView 4.1 program packages [20]. The optimization of the compounds have been done using DFT method with functional B3LYP and basis set 6-311G (d,p) [16-18]. The frequency calculations were also performed using the same level of theory. The absence of imaginary harmonic frequencies confirms that the optimized structures are the global minimum energy conformations. The

assignments of the vibrational modes were done by using GAR2PED software [19]. In addition to this the electrostatic potential mapping surfaces (MEPS) and HOMO-LUMO scheme were also plotted for more clear presentation regarding the charge distributions and reactive site of the molecules by the same DFT/B3LYP/6-311G (d,p) method at the 0.02 isovalues and 0.0004 isodensity value.

4. Results and discussion:

4.1 Synthetic characterizations of compounds:

The analytical Data, Colour, Melting Point and Percentage Yield of H_3bpt, Hppta and Hdptt are shown in table [1] and NMR results are summarized as follow.

H_3bpt: ^{1}H NMR (DMSO-d_6, δ, ppm): [7.62 (2H), 7.35 (1H), 7.14 (2H)] phenyl ring; 11.84 (s, 3H, NH). ^{13}C NMR (DMSO-d_6, δ, ppm): 201.05 (>C=S), 163.90 (>C=O) and [144.58-123.27] phenyl ring.

Hppta: ^{1}H NMR (DMSO-d_6, δ, ppm): [7.68 (2H), 7.27 (1H), 7.12 (2H)] phenyl ring; 5.23 (1H, NH). ^{13}C NMR (DMSO-d_6, δ, ppm): [142.68-122.17] phenyl ring and [173.74 C(1), 152.94 C(2)] thiadiazole carbons.

Hdptt: ^{1}H NMR (DMSO-d_6, δ, ppm): [7.70 (2H), 7.43 (1H), 7.10 (2H)] phenyl ring; 8.46 (1H, NH). ^{13}C NMR (DMSO-d_6, δ, ppm): [143.63-121.79] phenyl ring and [201.07 C=S, 154.87 C2] triazole carbons.

4.2 Molecular Geometry: The optimized molecular structures of the compounds H_3bpt, Hppta and Hdptt are shown in figures S1 (a), (b) & (c) respectively (in supplementary part). The calculated bond distances and bond angles participating in the ring formation have been compared with that of experimental values observed for the structurally related compounds [21-23] and the results are given in table 2(a), (b). The slight deviations between the

calculated and experimental geometric parameters is due to the fact that the theoretical calculations belong to isolated molecule in gaseous phase while the experimental results belongs to molecule in solid state and the existence of the intermolecular interactions which connects the molecules together. Here, in our case the molecules in present study are not exactly same with those experimentally observed molecules, undertaken for comparisons. These are the main causes for such deviations. The Mulliken's charge on the atoms participating in the ring formation is listed in the table 2(c). The energies of optimized structures of H_3bpt, Hppta and Hdptt are -32087.877 eV, -30006.914 eV and -30007.445 eV respectively and the dipole moments (in Debye) are 1.1739 D, 3.1613 D and 5.1288 D respectively with same point groups C_1.

4.3 Molecular properties:

4.3.1 Molecular electrostatic potential (MEP) and Frontier molecular orbital (FMO) analysis:

The Molecular Electrostatic Potential (MEP) is the most useful to study structure-reactivity relationship of the molecules [24]. The molecular electrostatic potential (MEP) is related to the electronic density and a very useful descriptor for determining the sites for electrophilic attack and nucleophilic reaction as well as hydrogen-bonding interactions [25, 26]. The MEP maps of molecules H_3bpt, Hppta and Hdptt are shown in figures S1 (a), (b), & (c) (in supplementary part). The electrophilic attack is illustrated by red (negative) regions whereas nucleophilic reactivity is shown by the blue (positive) regions and the green region cover the parts of the molecule where electrostatic potentials are close to zero. In figure (1), the region for electrophilic attack(red) is mainly localized on the oxygen atom of benzoyl group and weak electrophilic attack(yellow) is localized on the sulphur atom of thiosemicarbazide group whereas the nucleophilic reactivity of the molecule is mainly localized on the surface of H atoms bound to nitrogen of thiosemicarbazide group in H_3bpt. After the ring formation

phenomenon, sites for electrophilic attack and nucleophilic reaction changed as shown in figure (1). In case of Hppta, the region for electrophilic attack (red) is localized on the nitrogen atoms of thiadiazole ring, whereas the nucleophilic reactivity is localized on the surface of H atoms bound to nitrogen of amine group. Similarly the region for electrophilic attack (red+yellow) is localized on the sulphur atom of 1,2,4-triazole-3-thione ring and weak electrophilic attack(yellow) is localized on the nitrogen atom (free from H) of 1,2,4-triazole ring, whereas the nucleophilic reactivity is localized on the surface of H atoms bound to nitrogen of 1,2,4-triazole ring in Hdptt. The frontier molecular orbital can offer a reasonable qualitative prediction of the excitation properties. The energy gap between HOMO and LUMO is a critical parameter to predict molecular electrical transport properties. The HOMO energy characterizes the electron donating ability and the LUMO energy characterizes the electron accepting ability, and the HOMO-LUMO energy gap characterizes the molecular chemical stability and this energy gap are also responsible for spectroscopic properties of the molecules [27-28]. The energies of the HOMO and LUMO orbitals of molecules H_3bpt, Hppta and Hdptt were investigated using the DFT/B3LYP method. Figure S2 (in supplementary part) shows the isodensity surface plots of HOMO and LUMO and energy excitation scheme from the ground state (HOMO) to the first excited state (LUMO). The electronic transition from the ground state to the excited state due to a transfer of electrons from the HOMO to LUMO levels is mainly due to $\pi\cdots\pi$ transition. The positive phases are red and the negative ones are green. The small energy gap of molecules is termed as soft while the large energy gaps are termed as hard molecules. The hardness value (η) of a molecule can be defined by the formula [28].

$$\eta = \{-\varepsilon_{HOMO} + \varepsilon_{LUMO}\}/2$$

where ε_{HOMO} and ε_{LUMO} are the energies of the HOMO and LUMO molecular orbitals. The soft molecules are high reactive, high polarisable and less stable than the hard ones because soft molecules need small energy for excitation.

4.3.2 Analysis of global and local reactivity descriptors:

The global chemical reactivity of molecules have been defined in terms of hardness (η), softness (S), chemical potential (μ), electronegativity (χ) and electrophilicity index (ω) and local reactivity has been defined in terms of Fukui function and the philicity [29-32]. Using Koopman's theorem for closed-shell molecules, η, S, μ, χ and ω are related as:

$$\eta = (I - A)/2$$

$$\mu = -(I + A)/2$$

$$\chi = (I + A)/2 \quad = -\mu$$

$$S = 1/\eta$$

$$\omega = \mu^2/2\eta$$

$I = -E_{HOMO}$ and $A = -E_{LUMO}$

where I and A are the ionization potential and electron affinity of the compounds. χ is the Mulliken electronegativity, because of the fundamental relationship to the chemical potential, therefore χ is a property of the entire molecule [31]. In the reference global chemical reactivity of molecules, the electrophilicity index (ω) is the most important descriptor. It is a measure of energy lowering due to maximal electron flow between donor and acceptor [30]. Thus global and local chemical reactivity descriptors of molecules are very useful parameters to define the intensity of chemical reactivity and site selectivity. Therefore by calculating these parameters, we can explain theoretically the biologically active properties of molecules. All the calculated values of ionization potential, electron affinity, hardness, potential, softness and electrophilicity index are shown in table 3.

4.4 FTIR and Raman band analysis:

We focused mainly on those vibrational modes of molecules that belong to the groups participating in the ring formation phenomenon. For clear presentation the spectra are presented in many wavenumber regions. A summary of these vibrational bands (Infrared and Raman) along with the DFT calculated bands with assignments for the molecules H_3bpt, Hppta and Hdptt are listed in table 4(a), (b) & (c) respectively.

N–H stretching Region:

The N–H stretching vibrations were observed only in experimental IR at 3451 cm^{-1} for H_3bpt, which was calculated theoretically at 3452 cm^{-1}. It disappeared in the Hppta and Hdptt as a result of removal of H atom from –N site due to ring formation of H_3bpt. It is a clear signature of cyclization of H_3bpt. There are three N-H groups in H_3bpt but only one IR band corresponding to $\nu(N_4\text{-}H_5)$ is observed. In Hppta, H_5-atom of $N_4\text{-}H_5$ is removed on ring formation and therefore the N-H stretching disappears. On the other hand, in Hdptt, other two H-atoms of N-H bond are removed due to ring formation. Normally, we should expect $\nu(N_7\text{-}H_8)$ to appear in Hppta and $\nu(N_4\text{-}H_5)$ in Hdptt. However, it does not appear in Hppta. This is the most probably due to the complex H-bonds [33-34]. This complex H-bonds is because of the formation of supramolecular architecture of molecules through intermolecular hydrogen bonding, therefore ν(N–H) bond is weakened and finally result no experimental wave number. But it appears at ~3663 cm^{-1} in case of Hdptt. This ν(N–H) band is calculated at 3635 and 3668 cm^{-1} by using DFT method for an isolated molecule of Hppta and Hdptt respectively in the gaseous phase.

C–H stretching Region:

This C–H stretching modes are indirectly affected due to ring formation. Small changes are therefore expected in ν(C-H) vibrations during H_3bpt → Hppta and H_3bpt → Hdptt conversions. There are two ν(C-H) Raman bands at 3181 and 3163 cm^{-1} of H_3bpt and no IR band. The ν(C-H) mode is Raman active and IR inactive in H_3bpt. Whereas in Hppta it is strong IR as well as Raman active; giving a number of IR bands at ~ 3232, 3210, 3190, 3179, 3164 and 3137 cm^{-1} and Raman bands at ~ 3220, 3237, 3295, 3200, 3168, 3144, 3100, 3066 and 3046 cm^{-1}. Like H_3bpt the ν(C-H) mode Raman active and IR inactive in Hdptt giving Raman bands at 3111, 3072, 3048 and 3033 cm^{-1}.

C=O stretching, N-H bending and C=N stretching Regions:

The *ν*(C=O) band is observed weakly at 1721 cm^{-1} in the Raman spectra of H_3bpt and it disappeared completely in Raman spectra of Hppta and Hdptt due to removal of H_2O after the ring formation of H_3bpt. The Raman bands at 1595 cm^{-1} and 1560 cm^{-1} and IR bands at 1598 cm^{-1} and 1553 cm^{-1} of H_3bpt are attributed to $\beta(N_{10}\text{-}H_{11}) + \beta(N_4\text{-}H_5)$ and $\beta(N_6\text{-}H_7)$ of thiosemicarbazide group of H_3bpt. After the ring formation during H_3bpt → Hppta and H_3bpt → Hdptt conversions, the two Raman bands corresponding to $\beta(N_{10}\text{-}H_{11})$ plus $\beta(N_4\text{-}H_5)$ and $\beta(N_6\text{-}H_7)$ of thiosemicarbazide group and IR bands at ~1598 cm^{-1} [$\beta(N_{10}\text{-}H_{11})$] are disappeared whereas IR band at ~ 1553 cm^{-1} is red shifted to ~ 1534 cm^{-1} with small contribution of $\beta(N_6\text{-}H_7)$. This red shift is due to new vibrational mode; $\nu(C_2{=}N_3)+\nu(C_5{=}N_4)$, a characteristic band of thiadiazole ring. Further we observed a Raman band at 1519 cm^{-1} and an IR band at 1513 cm^{-1} assigned as $\nu(C_2{=}N_3)$ [thd], which give the clear evidence of ring formation and converted into the thiadiazole ring. Similarly in the spectral analysis Hdptt, the bands corresponding to $\beta(N_{10}\text{-}H_{11})$ plus $\beta(N_4\text{-}H_5)$ and $\beta(N_6\text{-}H_7)$ of thiosemicarbazide group/chain are disappeared in IR as well as Raman spectra. But a sharp Raman band at ~1583 cm^{-1} and a IR band at ~1585 cm^{-1} are appeared due to $\nu(C_2{=}N_3)$, a

characteristic band of triazole ring [trz]. The IR band at ~1492 cm^{-1} of Hdptt is attributed to $\beta(N_4\text{-}H_5)$. A single band at 1428 cm^{-1} in IR spectra and couple of Raman bands at 1443 cm^{-1} and 1453 cm^{-1} of Hdptt are appeared newly. On the basis of DFT calculation these bands are assigned as mixed contribution of $\nu(C_2{=}N_8)$ and $\tau(R_{trz})$ which give the clear evidence of ring formation and converted into the triazole ring. The bands define the existence of thiosemicarbazide group/chain i.e. characteristic bands, appeared at ~ 1407 cm^{-1} (strong) in Raman and at ~1406 cm^{-1} in IR spectra of H_3bpt and these are assigned as contribution of total possible vibrational modes thiosemicarbazide group/chain as shown in table 4 (a). These bands are completely disappeared in Raman as well as in IR spectra of both Hppta and Hdptt. This confirms that no more existence of thiosemicarbazide group/chain with aid of acid or base and ring formation of H_3bpt resulting Hppta and Hdptt.

C-N, C-S and N-N stretching Regions:

In the vibrational spectral analysis of H_3bpt, we observed a Raman band at ~1380 cm^{-1} and corresponding an IR band at 1383 cm^{-1}, attributed to $\nu(C_8\text{-}N_{10})+ \nu(C_8\text{-}N_6)$ and $\nu(C_8\text{-}S_9)$. Subsequently, a Raman band at ~1308 cm^{-1} and an IR band at ~1307 cm^{-1} are also appeared due to mixed contribution of vibrational modes of thiosemicarbazide + C=O + C=C as shown in table 4(a). These are the characteristic modes to define the open character of thiosemicarbazide in H_3bpt. But these bands are completely diminished in the Raman as well as in IR spectra after the ring formation of H_3bpt and change into the thiadiazole ring (Hppta) and triazole-thione ring (Hdptt) on the removal of water molecule in both cases. Since (C-N)+(N-H) bonds [figure 1(a), (b) & (c)] present in all the three molecules, therefore there is certain possibility to show the effect of red shift or blue shift due to the change in structure and thus due to change in the charge distribution. In this reference , we observed that the Raman band at ~1246 cm^{-1} and IR band at ~1254 cm^{-1} [$\nu(C_{12}\text{-}N_{10})+\beta(N_{10}\text{-}$

H_{11})] of H_3bpt is red shifted in case of Hppta, at ~1243 cm^{-1}(Raman) and 1247 cm^{-1}(IR) [$\nu(C_9\text{-}N_7)+\beta(N_7\text{-}H_8)$] respectively. Whereas in case of Hdptt, a Raman band (1267 cm^{-1}) and an IR(1270 cm^{-1}) are appeared with vibrational modes of triazole ring [$\nu(C_6\text{-}N_4)+\nu(N_4\text{-}N_3)$] and $\beta(N_4\text{-}H_5)$ with $\nu(C_6\text{-}S_7)$ as given in table 4 (b) & (c). Further, we observed stretching modes of (N-N) present in the thiadiazole ring of Hppta and triazole ring of Hdptt most significantly, which are the characteristic modes of ring formed. In the Raman spectra of Hppta, two bands at ~ 1149 cm^{-1} and 1103 cm^{-1} are assigned as ν(N-N), whereas in the IR spectra these two are appeared at ~1141 cm^{-1} and 1100 cm^{-1}. Similarly, In the Raman spectra of Hdptt, two bands at ~ 1154 cm^{-1} and 1120 cm^{-1} are assigned as ν(N-N), whereas in the IR spectra these are appeared at ~1146 cm^{-1}, 1116, and 1102 cm^{-1}.

Low wavenumber Regions:

This section contains mainly bending types of the vibartional modes viz. bending (–out of plane, -in plane, linear), scissoring, torsion, deformation, rocking and puckering with very small contribution of stretching modes of [thiosemicarbazide + (C=O)] group. The prominent Raman band at ~ 931 cm^{-1}/ IR band at ~ 934 cm^{-1} associated with various bending type vibrations of linking chain between two benzene rings [table 4(a)] is characteristic of H_3bpt, which also disappeared in Hppta and Hdptt (Fig.1). The region 900 – 650 cm^{-1} mainly belongs to the vibrational modes of β_{OUT}(C-H) of the benzene ring. But in addition to β_{OUT}(C-H), the bands corresponding to the vibrational modes of β(C=O), β(C-S), ν(C-S), deformation of (C-N-N) bond and ring puckering of benzene ring are observed significantly as listed in table 4(a). The ring closure in H_3bpt influences the band shape of benzene ring modes because of charge shift in the process to attain new stable configuration; Hppta and Hdptt. Subsequently, the lower wavenumber region 550-200 cm^{-1} belongs to the torsion modes of ring. Two Raman at 459 cm^{-1}, 236 cm^{-1} and IR band at 459 cm^{-1} are

attributed to torsion modes of benzene and thiadiazole rings in the spectra of Hppta [table 4(b)]. Similarly the Raman bands at 408 cm^{-1}, 362 cm^{-1}, 337 cm^{-1} and 324 cm^{-1} are assigned as torsion modes of benzene and trizole rings [table4(c)]. Before the ring formation in H_3bpt, these bands are observed at 423 cm^{-1} and 412 cm^{-1} in the IR spectra of H_3bpt and assigned as shown in table 4(a). However corresponding to these modes, no Raman band is appeared. In the Raman spectra of H_3bpt, three marker bands are observed at 327 cm^{-1}, 273 cm^{-1} and 238 cm^{-1}, which give the clear Raman signature of the presence of open chain character [thiosemicarbazide + (C=O)] of H_3bpt. The bands at 327 cm^{-1}, 273 cm^{-1} and 238 cm^{-1} are assigned as given in table 4(a). Since [thiosemicarbazide + (C=O)] of H_3bpt converted in thiadiazole and triazole-thione rings respectively in Hppta and Hdptt after removal of water molecule, therefore the Raman bands at 327 cm^{-1}, 273 cm^{-1} and 238 cm^{-1} of H_3bpt disappeared and new bands appeared corresponding to the modes of thiadiazole and triazole-thione rings.

5. Conclusions

The present work reports synthesis and spectroscopic studies of three compounds. It has been observed that on treatment of 1-benzoyl-4-phenyl-3-thiosemicarbazide with acid/ base followed by neutralisation process with base/ acid, thiosemicarbazide group is able to cyclise in two different ways leading to formation of thiadiazole and triazole rings. The cyclization is well characterized by FT-IR, Raman and DFT study. The cyclization is confirmed by disappearance of many bands belonging to the open chain subgroups of H_3bpt such as; N-H stretching, N-H bending, C-N stretching, N-H puckering, C=O stretching etc. The cyclization of thiosemicarbazide group of H_3bpt has also been confirmed by the appearance of many bands belonging to thiadiazole and triazole rings of resulting compounds Hppta and Hdptt respectively. The calculated geometrical parameters of each

compounds using DFT/B3LYP/6-311G(d,p) method are found in nice agreement with experimental results. The MEP and FMO analysis were done by the same DFT method. In addition to this, the global chemical reactivity of molecules has also been investigated. The energies of HOMO and LUMO are negative, which indicate that all are the stable compounds.

Acknowledgement

PG (Junior Research Fellow) and Om Prakash are grateful to the UGC, India for providing research fellowship. RKS is grateful to AvH Foundation, Germany, and DST and CSIR, New Delhi for support to procure micro-Raman setup. Authors are also grateful to biophysics lab; department of Physics and department of Chemistry, BHU, Varanasi-221005, for providing lab facilities.

References:

[1] J.J.R. Frausto da Silva, R.J.P. Williams, The Biological Chemistry of the Elements: The Inorganic Chemistry of Life, Oxford University Press, 16-Aug-2001

[2] S.-M. Lu, H. Alper, Intramolecular Carbonylation Reactions with Recyclable Palladium-Complexed Dendrimers on Silica: Synthesis of Oxygen, Nitrogen, or Sulfur-Containing Medium Ring Fused Heterocycles, J. Am. Chem. Soc. 127 (2005) 14776-14784.

[3] J. A. Joule, K. Mills, Heterocyclic Chemistry, 4th ed., Blackwell, Oxford, 2000.

[4] A.A. Geronikaki, J.C. Dearden, D. Filimonov, I. Galaeva, T.L. Garibova, T. Gloriozova, V. Krajneva, A. Lagunin, F.Z. Macaev, G. Molodavkin, V.V. Poroikov, S.I. Pogrebnoi, F. Shepeli, T.A. Voronina, M. Tsitlakidou, L. Vlad, Design of New Cognition Enhancers: From Computer Prediction to Synthesis and Biological Evaluation, J. Med. Chem. 47 (2004) 2870-2876.

[5] Z.-Y.J. Zhan, P.B. Dervan, alternative heterocycles for dna recognition: a 3-pyrazole/pyrrole pair specifies for g·c base pairs, Bioorg. Med. Chem. 8 (2000) 2467-2474.

[6] M. Bujard, V. Gouverneur, C. Mioskowski, A Highly Efficient and Practical Synthesis of Cyclic Phosphinates Using Ring-Closing Metathesis, J. Org. Chem. 64 (1999) 2119-2123.

[7] C.N. Hodge, J. Pierce, A diazine heterocycle replaces a six-membered hydrogen-bonded array in the active site of scytalone dehydratase, Bioorg. Med. Chem. Lett. 3 (1993) 1605-1608.

[8] C.S. Cooper, P.L. Klock, D.T.W. Chu, P.B. Fernandes, The synthesis and antibacterial activities of quinolones containing five- and six-membered heterocyclic substituents at the 7-position, J. Med. Chem. 33 (1990) 1246-1252.

[9] K.P. Boegesoe, J. Arnt, V. Boeck, A.V. Christensen, J. Hyttel, K.G. Jensen, Antihypertensive activity in a series of 1-piperazino-3-phenylindans with potent 5-HT2-antagonistic activity, J. Med. Chem. 31 (1988) 2247-2256.

[10] D. Ferraris, R.P. Ficco, T. Pahutski, S. Lautar, S. Huang, J. Zhang, V. Kalish, Design and synthesis of poly(ADP-ribose)polymerase-1 (PARP-1) inhibitors. Part 3: In vitro evaluation of 1,3,4,5-Tetrahydro-benzo[c][1,6]- and [c][1,7]-naphthyridin-6-ones, Bioorg. Med. Chem. Lett. 13 (2003) 2513-2518.

[11] N. Demirbas, S.A. Karaoglu, A. Demirbas, K. Sancak, Synthesis and antimicrobial activities of some new 1-(5-phenylamino-[1,3,4]thiadiazol-2-yl)methyl-5-oxo-[1,2,4]triazole and 1-(4-phenyl-5-thioxo-[1,2,4]triazol-3-yl)methyl-5-oxo- [1,2,4]triazole derivatives, Eur. J. Med. Chem. 39 (2004) 793-804.

[12] J. Matysiak, A. Nasulewicz, M. Pełczyńska, M. Świtalska, I. Jaroszewicz, A. Opolski, Synthesis and antiproliferative activity of some 5-substituted 2-(2,4-dihydroxyphenyl)-1,3,4-thiadiazoles, Eur. J. Med. Chem. 41 (2006) 475-482.

[13] A. Foroumadi, S. Emami, A. Hassanzadeh, M. Rajaee, K. Sokhanvar, M.H. Moshafi, A.

Shafiee, Synthesis and antibacterial activity of N-(5-benzylthio-1,3,4-thiadiazol-2-yl) and N-(5-benzylsulfonyl-1,3,4-thiadiazol-2-yl)piperazinyl quinolone derivatives,
Bioorg. Med. Chem. Lett. 15 (2005) 4488-4492.

[14] F. Clerici, D. Pocar, M. Guido, A. Loche, V. Perlini, M. Brufani, Synthesis of 2-Amino-5-sulfanyl-1,3,4-thiadiazole Derivatives and Evaluation of Their Antidepressant and Anxiolytic Activity, J. Med. Chem. 44 (2001) 931-936.

[15] A. Bharti, P. Bharati, R. Dulare, M.K. Bharty, D.K. Singh, N.K. Singh, Studies on phenylmercury(II) complexes of nitrogen–sulfur ligands: Synthesis, spectral, structural characterization, TD-DFT and photoluminescent properties,
Polyhedron, 65 (2013) 170-180.

[16] A. Bharti, M.K. Bharty, S. Kashyap, U.P. Singh, R.J. Butcher, N.K. Singh, Hg(II) complexes of 4-phenyl-5-(3-pyridyl)-1,2,4-triazole-3-thione and 5-(4-pyridyl)-1,3,4-oxadiazole-2-thione and a Ni(II) complex of 5-(thiophen-2-yl)-1,3,4-oxadiazole-2-thione: Synthesis and X-ray structural studies,
Polyhedron, 50 (2013) 582-591.

[17] R. Dulare, S.K. Kushawaha, M.K. Bharty, N.K. Singh, Syntheses, spectral and crystallographic studies of novel monometallic Co(II) and Zn(II) complexes with phenyl-(5-pyridin-4-yl[1,3,4]thiadiazol-2-yl)-amine, J. Mol. Struct. 984 (2010) 96-101.

[18] M. Tanaka, M. Ubukata, T. Matsuo, K. Yasue, K. Matsumoto, Y. Kajimoto, T. Ogo, T. Inaba, ChemInform Abstract: One-Step Synthesis of Heteroaromatic-Fused Pyrrolidines via Cyclopropane Ring-Opening Reaction: Application to the PKCβ Inhibitor JTT-010, ChemInform, 39 (2008).

[19] S. Das, T. Asefa, Epoxide Ring-Opening Reactions with Mesoporous Silica-Supported Fe(III) Catalysts, ACS Catal 1 (2011) 502-510.

[20] A.-C. Albertsson, I.K. Varma, Recent Developments in Ring Opening Polymerization of

Lactones for Biomedical Applications, Biomacromolecules, 4 (2003) 1466-1486.

[21] A.D. Becke, J. Chem. Phys. 98 (1993) 5648-5652.

[22] C. Lee, W. Yang, R.G. Parr, Phys. Rev. B. 37 (1988) 785-789.

[23] M. Biczysko, P. Panek, V. Barone, Chem. Phys. Lett. 475 (2009) 105–110

[24] J.M.L. Martin, C. Van Alsenoy, GAR2PED, University of Antwerp. 1995

[25] M.J. Frisch, J.A. Pople, Gaussian 03, Revision A.1, Gaussian, Inc., Pittsburgh, 2003.

[26] L. Coghi, A.M.M. Lanfredi, A. Tiripicchio, Crystal and molecular structure of thiosemicarbazide hydrochloride, J. Chem. Soc., Perkin Trans. 2, (1976) 1808-1810.

[27] M. Ishankhodzhaeva, S.A. Kadyrova, M. Surazhskaya, N. Parpiev, P. Koz'min, Crystalline and Molecular Structure of 2-Amino-5-phenyl-1, 3, 4-thiadiazole, Russ. J. Org. Chem. 37 (2001) 721-723.

[28] T. Karakurt, M. Dinçer, A. Çetin, M. Sekerci, Molecular structure and vibrational bands and chemical shift assignments of 4-allyl-5-(2-hydroxyphenyl)-2,4-dihydro-3H-1,2,4-triazole-3-thione by DFT and ab initio HF calculations, Spectrochim. Acta, Part A, 77 (2010) 189-198.

[29] B. Galabov, S. Ilieva, G. Koleva, W.D. Allen, H.F. Schaefer Iii, P. von R. Schleyer, Structure–reactivity relationships for aromatic molecules: electrostatic potentials at nuclei and electrophile affinity indices, WIREs Comput. Mol. Sci., 3 (2013) 37-55.

[30] H. Roohi, A.-R. Nowroozi, E. Anjomshoa, H-bonded complexes of uracil with parent nitrosamine: A quantum chemical study, Comp. Theor. Chem. 965 (2011) 211-220.

[31] P. Munshi, T.N. Guru Row, Intra- and intermolecular interactions in small bioactive molecules: cooperative features from experimental and theoretical charge-density analysis, Acta Crystallogr.,Sect. B, 62 (2006) 612-626.

[32] M. Belletête, J.-F. Morin, M. Leclerc, G. Durocher, A Theoretical, Spectroscopic, and Photophysical Study of 2,7-Carbazolenevinylene-Based Conjugated Derivatives,

J. Phys. Chem. A, 109 (2005) 6953-6959

[33] D. Zhenming, S. Heping, L. Yufang, L. Diansheng, L. Bo, Experimental and theoretical study of 10-methoxy-2-phenylbenzo[h]quinoline, Spectrochim. Acta, Part A, 78 (2011) 1143-1148.

[34] K. Fukui, Role of Frontier Orbitals in Chemical Reactions, Science, 218 (1982) 747-754.

[35] R.G. Parr, L.v. Szentpály, S. Liu, Electrophilicity Index, J. Am. Chem. Soc. 121 (1999) 1922-1924.

[36] R.G. Parr, R.A. Donnelly, M. Levy, W.E. Palke, Electronegativity: The density functional viewpoint, J. Chem. Phys. 68 (1978) 3801-3807.

[37] R.G. Pearson, Chemical hardness and density functional theory, J. Chem. Sci., 117 (2005) 369.

[38] J.C. Pedregosa, G. Alzuet, J. Borras, S. Fustero, S. Garcia-Granda, M.R. Diaz, Acta Crystallogr., C49 (1993) 630.

[39] O. Prakash, S.K. Singh, B. Singh, R.K. Singh, Investigation of coordination properties of isolated adenine to copper metal: A systematic spectroscopic and DFT study, Spectrochim. Acta, Part A, 112 (2013) 410–416.

Figure Captions:

Figure 1(a): Optimized structure and MEP surface map of H_3bpt.

Figure 1(b): Optimized structure and MEP surface map of Hppta.

Figure 1(c): Optimized structure and MEP surface map of Hdptt.

Figure 2: The HOMO-LUMO plots for the (a) H_3bpt, (b) Hppta and (c) Hdptt.

Figure 3(a): Experimental FT-IR and Raman spectra of H_3bpt.

Figure 3(b): Experimental FT-IR and Raman spectra of Hppta.

Figure 3(c): Experimental FT-IR and Raman spectra of Hdptt.

Tables Captions:

Table 1: Analytical Data: Empirical formulae, Color, Melting Point, & Percentage Yield of H_3bpt, Hppta and Hdptt and elemental analysis.

Table 2(a): Selected bond lengths of H_3bpt, Hppta and Hdptt calculated by DFT method with experimental results [21, 22 and 23].

Table 2(b): Selected bond angles of H_3bpt, Hppta and Hdptt calculated by DFT method with experimental results [21, 22 and 23].

Table 2(c): Mulliken's charge on the selected atoms of of H_3bpt, Hppta and Hdptt calculated by DFT method.

Table 3: Global reactivity descriptors and other parameters related to molecular properties calculated by DFT method:

Table 4(a): Calculated and experimental wavenumbers (in cm^{-1}) and their tentative vibrational assignments[a] (PED) of H_3bpt. (wavenumbers less than 200 cm^{-1} are not included):

Table 4(b): Calculated and experimental wavenumbers (in cm^{-1}) and their tentative vibrational assignments[a] (PED) of Hppta. (wavenumbers less than 200 cm^{-1} are not included):

Table 4(c): Calculated and experimental wavenumbers (in cm^{-1}) and their tentative vibrational assignments[a] (PED) of Hdptt. (wavenumbers less than 200 cm^{-1} are not included):

Figure 1

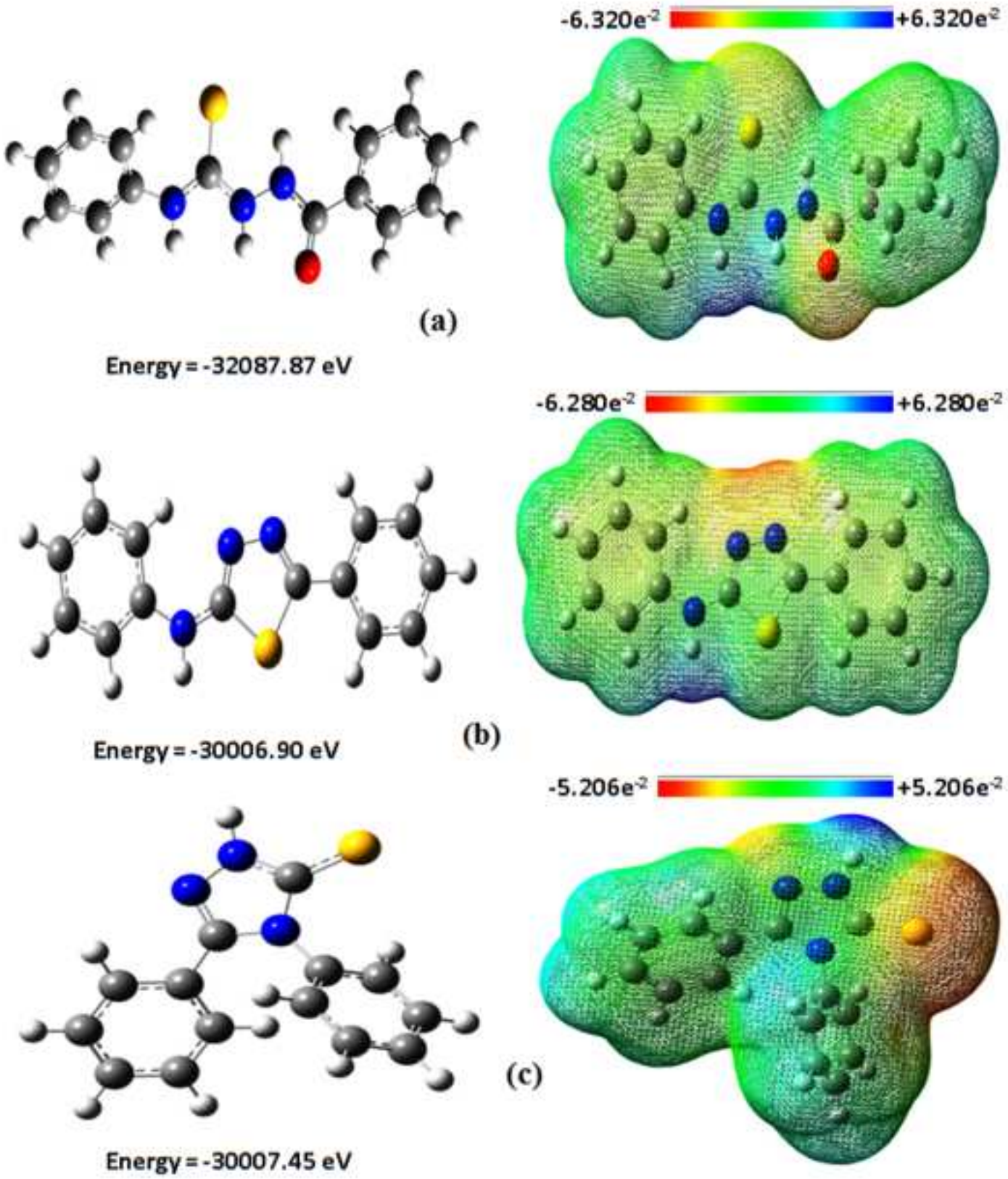

Figure (1) Optimized structures and MEP surface maps of (a)H_3bpt, (b) Hppta and (c) Hdptt

Figure 2

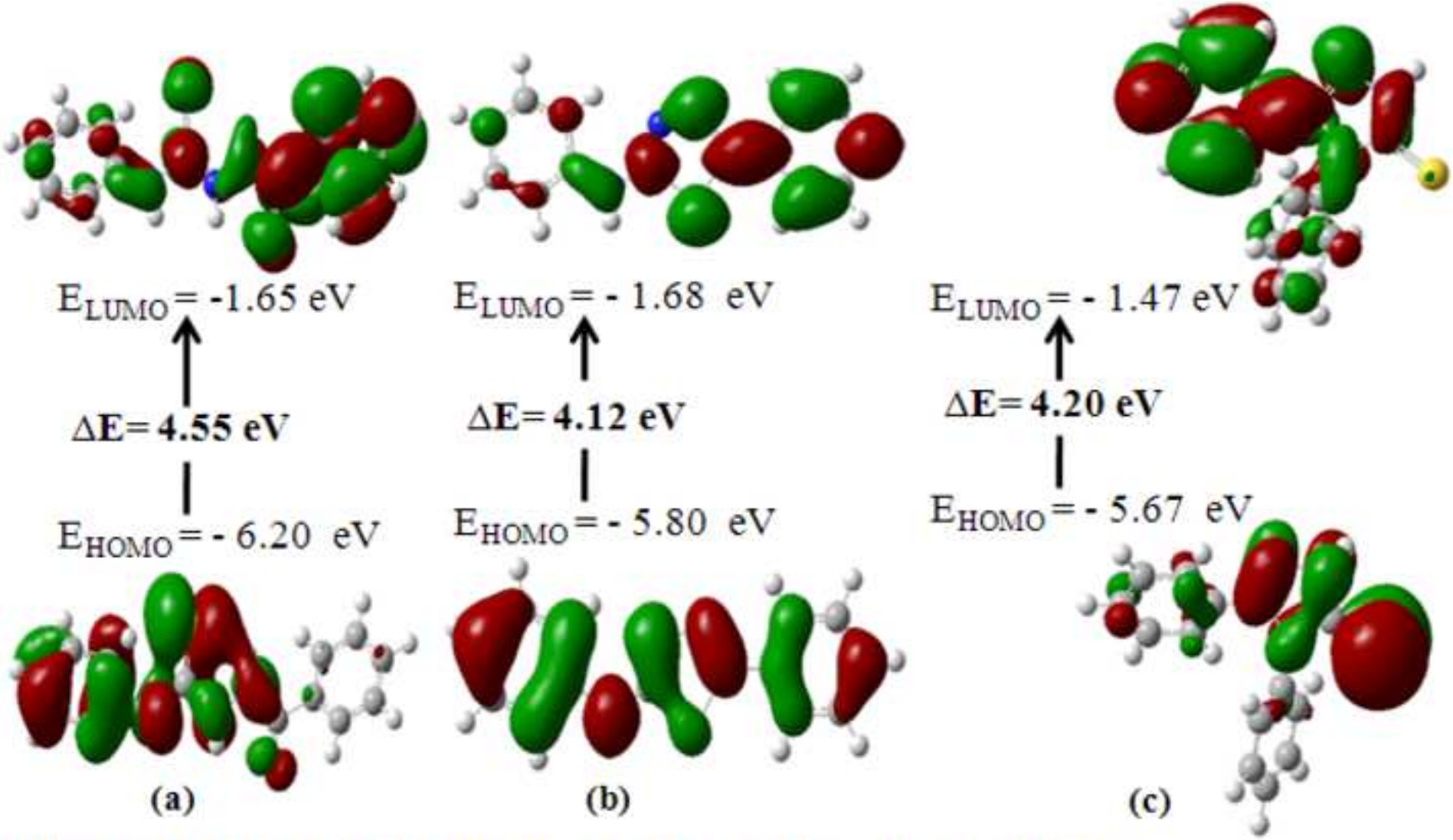

Figure (2) HOMO-LUMO plots for (a) H_3bpt, (b) Hppta and (c) Hdptt

Figure 3(a)

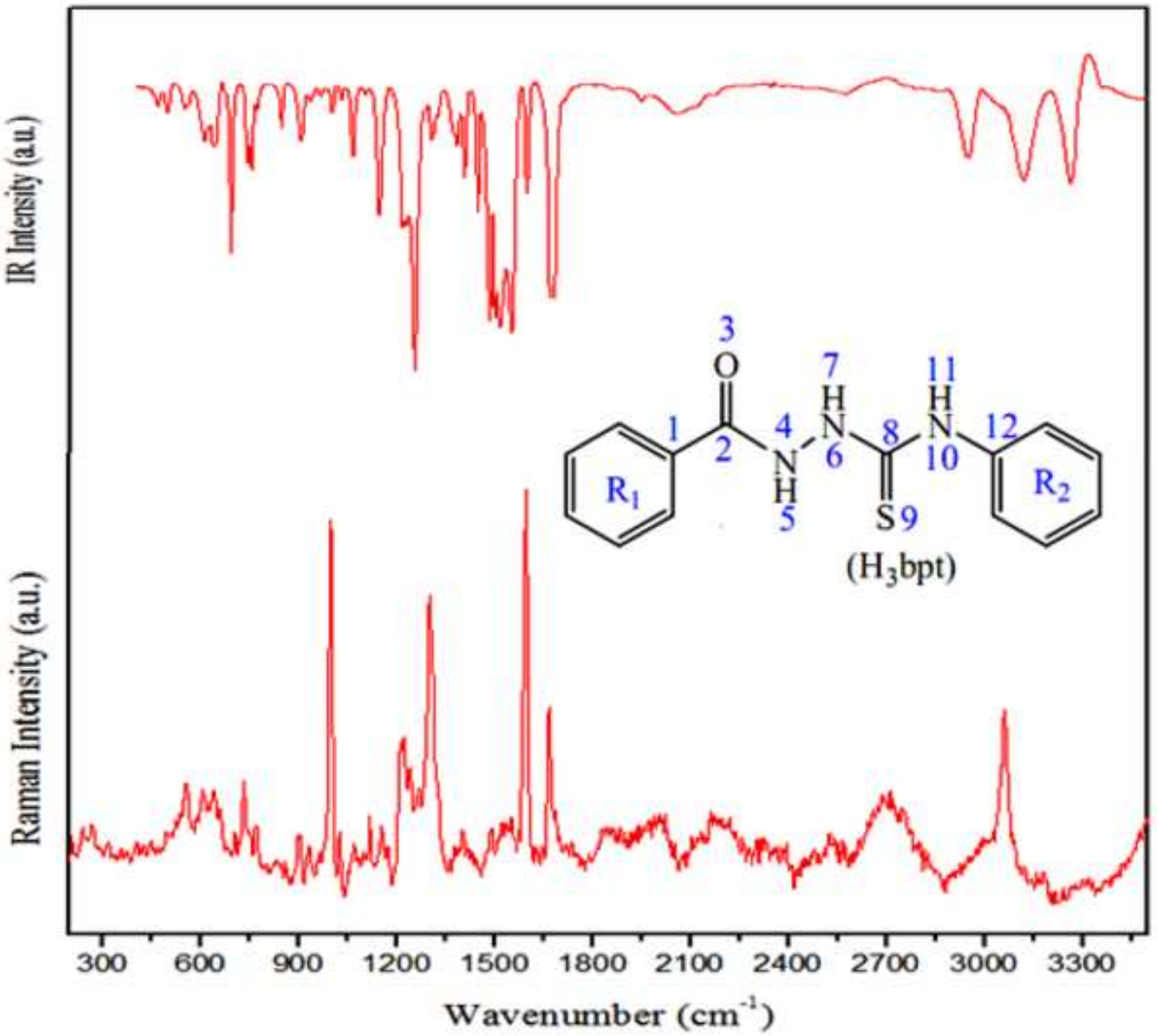

Figure 3(b)

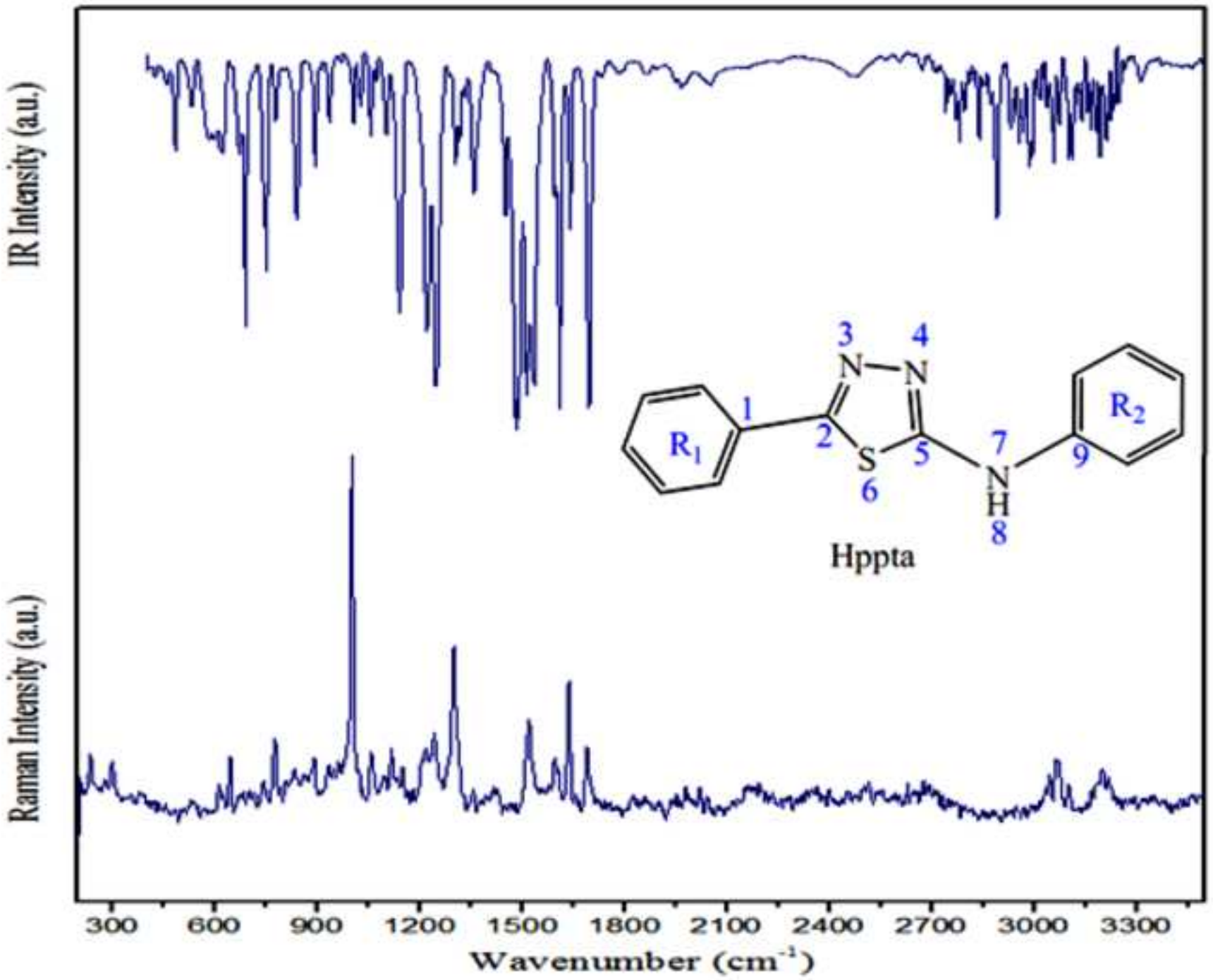

Figure 3(c)

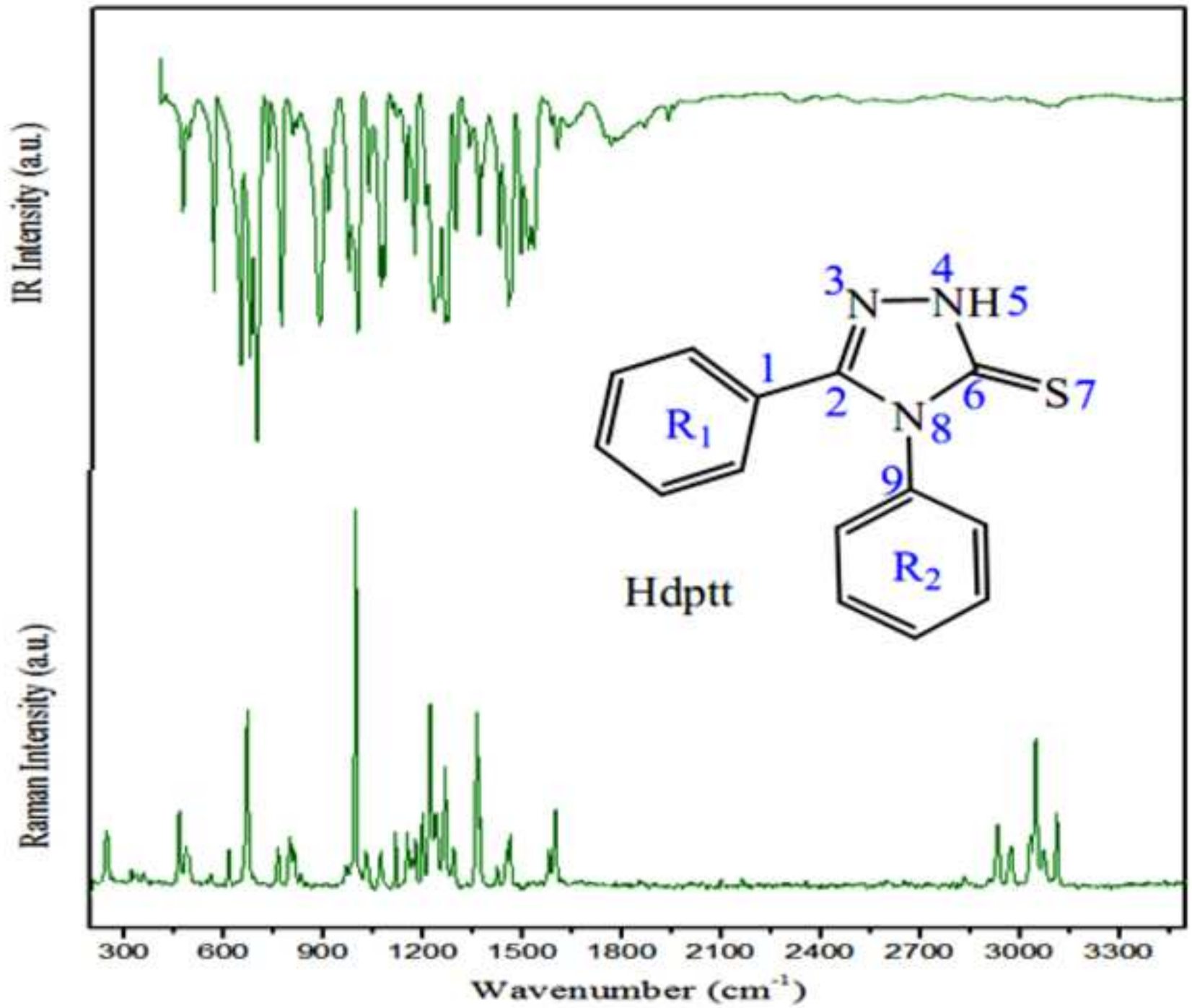

Table 1:

S. No.	Empirical formula (Weight in gm.)	M.P.(^{0}C)	Color	Yield (%) (gm)	Elemental Analysis %Found (calc.)			
					C	H	N	S
(1)	$C_{14}H_{13}N_3SO$ (281.34)	142	White	86	59.75 (59.77)	4.68 (4.66)	18.47 (18.50)	11.38 (11.36)
(2)	$C_{14}H_{11}N_3S$ (263.33)	176	Dirty white	78	63.88 (63.86)	4.23 (4.21)	19.79 (19.75)	12.20 (12.18)
(3)	$C_{14}H_{11}N_3S$ (263.33)	214	Yellow	82	63.90 (63.86)	4.22 (4.21)	19.77 (19.75)	12.21 (12.18)

Table 2(a)

No.	H_3bpt	Calc.	Expt.(21)	Hppta	Calc.	Expt.(22)	Hdptt	Calc.	Expt.(23)
1.	N_4-H_5	1.019	l.000	C_2-N_8	1.396	1.372	C_2-S_6	1.778	1.729
2.	N_4-N_6	1.388	1.418	C_2=N_3	1.304	1.300	C_2=N_3	1.295	1.291
3.	N_6-H_7	1.018	0.910	C_6-N_8	1.396	1.367	C_5=N_4	1.304	1.309
4.	N_6-C_8	1.366	1.363	C_6-N_4	1.357	1.329	C_5-S_6	1.769	1.741
5.	S_9-C_8	1.680	1.692	C_6-S_7	1.667	1.679	C_5-N_7	1.365	1.353
6.	C_8-N_{10}	1.370	1.314	N_4-N3	1.362	1.375	N_4-N_3	1.360	1.388
7.	N_{10}-H_{11}	1.011	0.860	N_8-C_9	1.434	1.466	C_9-N_7	1.409	1.415
8.	C_1-C_2	1.490		C_2-C_1	1.470	1.472	N_7-H_8	1.007	
9.	C_{12}-N_{10}	1.415		H_5-N_4	1.007		C_2-C_1	1.466	
10.	C_2-N_4	1.372							
11.	C_2=O_3	1.226							

Table 2(b)

No.	H_3bpt	Calc.	Expt.(21)	Hppta	Calc.	Expt.(22)	Hdptt	Calc.	Expt.(23)
1.	N_4-N_6-H_7	109.92	1 13.00	N_3=C_2-C_1	122.46	125.06	C_2-S_6-C_5	85.81	87.5
2.	N_6-C_8-N_{10}	111.14	114.50	N_8-C_2-C_1	126.89	124.23	C_5=N_4-N_3	112.81	111.8
3.	H_5-N_4-N_6	111.79	116.00	C_2-N_8-C_9	127.79	127.23	N_4=C_5-S_6	113.76	113.4
4.	C_8-N_{10}-H_{11}	114.74	114.00	N_4-C_6-S_7	127.95	128.74	C_2=N_3-N_4	115.06	114.0
5.	N_4-N_6-C_8	120.31	139.20	N_8-C_6-S_7	130.12	127.30	S_6-C_5-N_7	119.8	120.5
6.	N_6-C_8-S_9	121.74	121.00	N_8-C_6-N_4	101.93		N_4=C_5-N_3	126.45	126.1
7.	H_7-N_6-C_8	122.56	117.00	C_2=N_3-N_4	104.59		C_5-N_7-C_9	129.56	128.0
8.	S_9-C_8-N_{10}	127.06	124.50	C2-N_8-C_6	108.05		N_3=C_2-S_6	112.56	
9.	C_{12}-N_{10}-H_{11}	113.59		N_8-C_2=N_3	110.65		C_9-N_7-H_8	114.73	
10.	C_2-N_4- N_6	115.65		C_6-N_4-N_3	114.79		C_5-N_7-H_8	115.71	
11.	C_1-C_2-N_4	116.01		H_5-N_4-N_3	120.73		C_1-C_2-S_6	123.14	
12.	N_4-C_2 =O_3	120.31		C_6-N_8-C_9	123.82		N_3=C_2-C_1	124.3	
13.	C_1-C_2=O_3	123.66		C_6-N_4-H_5	124.48				
14.	C_2-N_4- H_5	124.44							
15.	C_{12}-N_{10}-C_8	130.72							

Table 2(c)

No.	H_3bpt	Charge	Hppta	Charge	Hdptt	Charge
1.	N_{10}	-0.457	N_7	-0.473	S_7	-0.242
2.	H_{11}	0.226	H_8	0.237	C_6	0.154
3.	C_8	0.208	C_5	0.219	N_4	-0.243
4.	S_9	-0.252	S_6	0.181	H_5	0.269
5.	N_6	-0.272	C_2	-0.003	N_3	-0.205
6.	H_7	0.242	N_3	-0.190	C_2	0.368
7.	N_4	-0.284	N_4	-0.242	N_8	-0.459
8.	H_5	0.269	C_1	-0.064	C_9	0.057
9.	C_2	0.451	C_9	0.167	C_1	-0.134
10.	O_3	-.0394				
11.	C_1	-0.189				
12.	C_{12}	0.186				

Table 3:

Molecular Properties	H_3bpt	Hppta	Hdptt
Ionization potential (I)	6.20	5.67	5.80
Electron affinity (A)	1.65	1.47	1.68
Global hardness(η)	2.275	2.1	2.06
Global softness (s)	0.440	0.476	0.486
Electronegativity (χ)	3.925	3.57	3.74
Chemical potential (μ)	-3.925	-3.57	-3.74
Global electrophilicity (ω)	3.386	3.035	3.395

Table 4(a)

Modes	Calculated frequencies	IR (cm^{-1})	Raman (cm^{-1})	Vibrational assignments with PED (≥ 4%)
Q 1	3574.86			$\nu(N_{10}\text{-}H_{11})(99)$
Q 2	3492.27			$\nu(N_6\text{-}H_7)(96)$- $\nu(N_4\text{-}H_5)(4)$
Q3	3452.07	3451		$\nu(N_4\text{-}H_5)(95)$- $\nu(N_6\text{-}H_7)(4)$
Q4	3234.30			ν(C-H)R2(98)
Q5	3204.26			ν(C-H)R1(97)
Q6	3193.56		3181	ν(C-H)R2(87)
Q7	3175.97			ν(C-H)R1(97)
Q8	3153.60		3163	ν(C-H)(98)
Q9	1715.98		1721	$\nu(C_2{=}O_3)(74)$+ $\rho(N_4\text{-}H_5)(6)$- $\nu(C_1\text{-}C_2)(5)$- $\nu(C_2\text{-}N_4)(5)$
Q10	1645.45	1674	1667	ν(C-C)R2(55)+ δ_{ASYM}R2(9)+ β(C-H)R2(6)
Q11	1577.07	1598	1595	$\beta(N_{10}\text{-}H_{11})(19)$- $\nu(C_8\text{-}N_6)(15)$- $\beta(N_6\text{-}H_7)(14)$ +$\beta(N_4\text{-}H_5)(10)$+ $\nu(C_8\text{-}N_{10})(18)$+ $\nu(N_4\text{-}N_6)(5)$- $\nu(C_2\text{-}N_4)(5)$
Q12	1562.27	1553	1560	$\beta(N_{10}\text{-}H_{11})(28)$+ $\beta(N_6\text{-}H_7)(16)$- $\beta(N_4\text{-}H_5)(12)$+ $\nu(C_2\text{-}N_4)(7)$
Q12	1526.33	1515	1533	β(C-H)R1(56)+ ν(C-C)R1(22)
Q14	1481.26	1484	1488	β(C-H)R1(36)+ ν(CC)R1(17)- β(C-H)R2(6)
Q15	1478.44	1447		β(C-H)R2(24)- ν(CC)R2(18)+ β(C-H)R1(7)- $\beta(N_{10}\text{-}H_{11})(5)$
Q16	1427.30	1406	1407	$\beta(N_4\text{-}H_5)(21)$+$\beta(N_6\text{-}H_7)(20)$-$\nu(C_2\text{-}N_4)(18)$+$\nu(C_8\text{-}N_6)(7)$- $\nu(C_8\text{-}N_{10})(6)$+ $\nu(C_1\text{-}C_2)(6)$
Q17	1373.88	1383	1380	$\nu(C_8\text{-}N_{10})(19)$+ β(C-H)R2(25)- $\nu(C_8\text{-}S_9)(10)$+ $\nu(C_8\text{-}N_6)(8)$
Q18	1309.14	1307	1308	$\nu(N_4\text{-}N_6)(23)$-$\nu(C_8\text{-}N_6)(12)$-$\beta(N_4\text{-}H_5)(8)$+$\nu(C_1\text{-}C_2)(8)$- $\rho(N_4\text{-}H_5)(7)$+$\delta(C_2N_4N_6)(7)$-$\beta(C_2{=}O_3)(6)$+$\nu(C_{12}\text{-}N_{10})(5)$
Q19	1251.63	1254	1246	$\nu(C_{12}\text{-}N_{10})(19)$- ν(CC)R2(24)+ $\beta(N_{10}\text{-}H_{11})(8)$- β(C-H)R2(6)+ δR2(6)
Q20	1205.20	1215		β(C-H)R2(47)- β(C-H)R1(15)
Q21	1184.34			β(C-H)R1(78)- ν(CC)R1(17)
Q22	1051.15	1065	1074	ν(CC)R2(53)+β(C-H)R2(16)- μR2(5)
Q23	1017.73	1002	1002	δ_{TRI}R1(56)-ν(CC)R1(35)
Q24	927.52	934	931	$\rho(N_4\text{-}H_5)(36)$+ $\delta(C_2N_4N_6)(36)$+$\beta(C_2{=}O_3)(11)$-$\delta(C_{12}N_{10}C_8)(5)$+ $LIN(N_4N_6C_8N_{10})$
Q25	876.20	872		ν(CC)R2(20)- δ_{TRI}R2(13)+$\nu(C_{12}N_{10})(11)$- $\nu(N_4N_6)(7)$-$\nu(N_6C_8)(6)$+δ_{ASYM}R2(5)- $\beta(C_2{=}O_3)(5)$- $\delta(C_{12}N_{10}C_8)(5)$
Q26	834.22	847	838	β_{OUT}(CH)R2(98)
Q27	774.35	774	775	μR2(27)-β_{OUT}(CH)R2(26)- $\beta_{OUT}(C_{12}\text{-}N_{10})(19)$+ $\delta(C_{12}N_{10}C_8)(6)$+ δ(CCC)R2(5)
Q28	724.97		731	β_{OUT}(CCN)R1(16)+$\nu(S_9C_8)(10)$-β_{OUT}(CH)R1(35)-δ_{ASYM}R1(7)-$\delta(N_4N_6C_8)(6)$+
Q29	698.90	692		μR2(57)+β_{OUT}(CH)R2(16)- β_{OUT}(CCC)R2(6)
Q30	670.70	692		δ_{ASYM}R1(22)+$\beta(C_2{=}O_3)(12)$-$\delta(C_8N_6N_4)(11)$+$\delta(C_{12}N_{10}C_8)(7)$+ δ_{ASYM}R2(7)+$\nu(S_9C_8)(6)$+$\beta(S_9C_8)(6)$
Q31	631.60	635	641	δ_{ASYM}R2(81)
Q32	592.32			$\beta_{OUT}(N_6C_8N_{10})(57)$- $W(H_5N_4)(8)$-$\tau(C_2\text{-}N_4)(7)$
Q33	483.91	496		$\beta_{OUT}(N_6\text{-}H_7)(15)$-$\tau(C_8\text{-}N_6)(14)$+$\tau(N_4\text{-}N_6)(11)$+$\tau(C_8\text{-}N_{10})(9)$-$\tau_{ASYM}$R2(8)- $\beta_{OUT}(N_{10}H_{11})(6)$+$\beta_{OUT}[N_{31}CC(R2)](5)$-$\tau(C_{12}\text{-}N_{10})(5)$
Q34	464.71	469		$\beta_{OUT}(N_6H_7)(22)$+$\beta_{OUT}(N_{10}H_{11})(11)$+$\tau(N_6\text{-}N_4)(10)$-$\tau(C_8\text{-}N_6)(9)$- $\tau(C_2\text{-}N_4)(6)$-$\tau(C_8\text{-}N_{10})(6)$-$\tau_{ASYM}$R1(5)
Q35	438.51	423		τ_{ASYM}R1(39)+$\beta_{OUT}[C_{23}CC(R1)](19)$- $\beta(N_4H_5)(6)$
Q36	417.26	412		δ_{ASYM}R2(83)
Q37	342.19		327	$\beta(C_{12}\text{-}N_{10})(29)$-$\delta(C_2N_4N_6)(10)$+$LIN(N_4N_6C_8N_{10})(7)$-$\tau(C_8N_6)(6)$ -$\beta_{OUT}(N_4H_5)(5)$-$\beta_{OUT}(N_4N_6C_8)(5)$
Q38	275.82		273	$LIN(N_4N_6C_8N_{10})(26)$-$\beta(S_9C_8)(12)$+$\delta(C_2N_4N_6)(10)$ +$\beta_{OUT}(N_4H_5)(9)$+τR1(8)
Q39	238.02		238	δ_{ASYM}R2(37)-$\delta(C_{12}N_{10}H_{11})(11)$+$LIN(N_4N_6C_8N_{10})(7)$- $\delta(H_5N_4N_6)(6)$+$\tau(C_8N_{10})(5)$

Table 4(b)

Modes	Calculated frequencies	IR (cm^{-1})	Raman (cm^{-1})	Vibrational assignments with PED (≥ 4%)
Q 1	3635.80			$\nu(N_7H_8)(100)$
Q 2	3234.10	3232	3237, 3220, 3295	ν(CH)R2(98)
Q3	3207.06	3210	3200	ν(CH)R1(98)
Q4	3191.37	3190		ν(CH)R1(95)
Q5	3177.57	3179		ν(CH)R2(92)
Q6	3169.83	3164	3168	ν(CH)R1(98)
Q7	3147.80	3137	314	ν(CH)(98)
Q8	1644.14	1696, 1641	1636,1657	ν(CC)R1(55)+ δ_{ASYM} R1(10)+ β(CH)R1(11)- β_{OUT}(CHC)R1(5)
Q9	1619.88	1610	1600, 1609	ν(CC)R1(66)+ β(CH)R1(10) +δ_{ASYM}R1(9)
Q10	1538.01	1534		$\nu(C_2{=}N_3)(19)+ \nu(C_5{=}N_4)(16)- \nu(C_2C_1)(11)- \beta(N_7H_8)(8)- \nu(C_5N_7)(6)+$ β(CH)R1(6)- ν(CC)R1(5)
Q11	1509.69	1513, 1491	1519	$\nu(C_2{=}N_3)(36)$-β(CH)R1(27)-ν(CC)R1(11)
Q12	1472.75	1451	1481	β(CH)R1(36)- ν(CC)R1(19)- $\nu(C_2{=}N_3)(9)$
Q13	1356.97	1359	1358	β(CH)R1(49)- $\beta_{OUT}R_{thd}(11)$- ν(CC)R1(23)
Q14	1341.86	1333	1330	ν(CC)R2(68)+ β(CH)R2(7)- $\nu(C_9N_7)(7)$
Q15	1327.53			ν(CC)R1(66)+ β(CH)R1(12)
Q16	1257.59	1247	1243	$\nu(C_9N_7)(28)$-ν(CC)R2(26)-$\beta(N_7H_8)(9)$+δ_{ASYM}R2(7)- β(CH)R2(7)- $\nu(C_5N_4)(6)$
Q17	1207.35	1220	1219, 1208	β(CH)R2(42)-β(CH)R2(34)+ν(CC)R2(10)
Q18	1183.78		1181	β(CH)R1(79)+ν(CC)R1(15)
Q19	1145	1141	1149 1136	$\nu(N_4N_3)(55)-\ \beta(C_5\text{-}N_7)(7)$
Q20	1102.20	1100	1119 1103	ν(CC)R1(34)- $\nu(N_4N_3)(12)$- β(CH)R1(24)
Q21	1052.78	1058	1060	ν(CC)R1(34)+ ν(CC)R2(22)
Q22	1015.50	1006	1003	μR1(68)-ν(CC)R1(19)
Q23	854.67	840	834	$\delta R_{thd}(22)$-$\nu(C_9N_7)(15)$+δ_{TRI}R2(11)-ν(CC)R2(21)+ $\nu(C_5S_6)(6)$+δ_{ASYM}R2(5)
Q24	825.30		810	$\beta_{OUT}(C_5N_7C_9)(33)$-$\beta(C_5\text{-}N_7)(15)$-$\nu$(CC)R2(7)-$\nu(N_4\text{-}N_3)(7)$- $\nu(C_5\text{-}S_6)(7)$+$\beta(C_9\text{-}N_7)(6)$
Q25	751.05		745	$\nu(C_5S_6)(25)$-$\nu(C_2S_6)(14)$-$\delta R_{thd}(11)$+ δ_{ASYM}R1(7)- $\delta(C_9N_7H_8)(5)$+$\nu(C_2C_1)(5)$
Q26	703.54		701	μR1(57)-β_{OUT}(CH)R1(28)+μR2(6)- β_{OUT}(CCC)R1(5)
Q27	686.26		685	δ_{ASYM}R1(42)+$\nu(C_2S_6)(28)$+$\beta(C_2C_1)(7)$+ν(CC)R1(5)
Q28	635.38		644	δ_{ASYM}R2(36)-δ'_{ASYM}R2(25)-δ_{ASYM}R1(18)
Q29	604.98		614	$\mu R_{thd}(20)$-$\delta R_{thd}(19)$+δ_{ASYM}R2(17)- δ_{ASYM}R1(11)+$\nu(C_2S_6)(9)$+$\nu(C_5S_6)(6)$+$\beta(C_2C_1)(5)$
Q30	592.13	600 581		δ_{ASYM}R2(39)-$(C_5S_6)(26)$-$\delta(C_9N_7H_8)(9)$+δ_{ASYM}R2(8)
Q31	514.27	532	533	$(C_9N_7)(35)$-δ_{ASYM}R2(24)-τ_{ASYM}R2(10)+β_{OUT}(CCC)R2(8)+ τ_{ASYM}R1(5)-μR2(5)
Q32	500.11	483 459	459	τ_{ASYM}R1(31)+$\beta_{OUT}[C_1CC(R1)](19)$-$\tau$Rthd(13)- $\beta_{OUT}(C_9N_7)(8)$+τ_{ASYM}R2(5)- β_{OUT}(CH)R1(5)
Q33	418.99	424		$\beta(C_2C_1)(21)$-$\beta(C_9N_7)(12)$-$\beta(C_5N_7)(8)$-$\nu(C_2S_6)(7)$-δ_{ASYM}R1(6)- $\beta(N_7H_8)(6)$
Q34	354.76		356	$\nu(C_2S_6)(20)$-δ_{ASYM}R1(9)+$\beta(C_2C_1)(8)$-$\nu(C_5S_6)(7)$+$\nu(C_2C_1)(7)$- $\delta R_{thd}(7)$-$\beta(C_9N_7)(6)$- $\beta(C_2C_1)(5)$-$\nu(C_9N_7)(5)$
Q35	284.57		302 280	$\beta(C_9N_7)(40)$+$\beta(C_5N_7)(29)$-$\beta(C_2C_1)(8)$-$\mu R_{thd}(3)$
Q36	234.68		236	τ'_{ASYM}R2(38)+μR1(12)-$\tau(C_5N_7)(7)$+β_{OUT}(CH)R2(6)+ $\tau(C_2N_3N_4C_5S_6)(6)$+$\beta_{OUT}(C_9N_7)(6)$-μR2(6)+τ_{ASYM}R1(5)+ $\tau(C_9N_7)(5)$

Table 4(c)

Modes	Calculated frequencies	IR (cm^{-1})	Raman (cm^{-1})	Vibrational assignments with PED (≥ 4%)
Q 1	3668.66	3663		$\nu(N_4\text{-}H_5)(99)$
Q 2	3206.44			$\nu(CH)R2(66)+ \nu(CH)R1(25)$
Q3				$\nu(CH)R2(93)$
Q4			3111,3072, 3048	$\nu(CH)R2(47)+ \nu(CH)R1(31)$
Q5	3178.35			$\nu(CH)R1(95)$
Q6	3170.20		3033	$\nu(CH)R2(95)$
Q7	1625.87	1632		$\nu(CC)R1(55)+ \beta(CH)R1(8)+\delta_{ASYM}R1(7)+ \nu(C_2=N_3)(7)$
Q8	1586.07	1585	1600 1583	$\nu(C_2=N_3)(48)- \nu(C_2C_1)(13)- \nu(CC)R1(8)$
Q9	1531.66	1531		$\beta(CH)R2(48)+\nu(CC)R2(29)+ \nu(N_8C_9)(8)$-
Q10	1489.63	1492		$\beta(N_4H_5)(15)+ \beta(CH)R2(20)- \nu(C_6H_4)(12)+ \nu(CC)R2(13)$
Q11	1476.91	1454,1461,		$\beta(CH)(43)- \nu(CC)R1(28)$
Q12	1406.65	1428	1443,1453	$\nu(C_2N_8)(33)- \nu(C_2C_1)(13)- \nu(C_9N_8)(13)+ \tau R_{trz}(9)- \beta(CH)R1(5)$
Q13	1352.85	1366		$\beta(CH)R2(42)- \nu(CC)R2(8)$
Q14	1340.39	1336		$\nu(C_9N_8)(16)\text{-}\nu(C_6N_8)(10)\text{-}\nu(CC)R2(21)\text{-}\delta_{ASYM}R_{trz}(9)\text{-}\nu(C_2=N_3)(7)\text{-}\beta(CH)R2(6)$
Q15	1325.92	1320		$\nu(CC)R2(67)+\beta(CH)R2(14)$
Q16	1261.19	1270	1267	$\nu(C_2N_5)(36)+ \beta(N_5H_4)(25)- \nu(C_2S_7)(10)+ \nu(N_5N_6)(7)$
Q17	1224.39	1229	1221	$\nu(C_6N_8)(36)- \tau R_{trz}(20)- \nu(C_6S_7)(12)- \nu(C_6N_4)(7)$
Q18	1208.31	1204		$\beta(CH)R1(68)+ \nu(CC)R1(15)$
Q19	1196.46		1200	$\beta(C_9H_{15})R2(78)+ \nu(CC)R2(12)$
Q20	1185.32	1173	1179	$\beta(CH)R1(72)+ \nu(CC)R1(15)$
Q21	1143.32	1146	1154	$\nu(N_4\text{-}N_3)(25)- \nu(C_2N_8)(23)+ \delta_{ASYM}R_{trz}(6)\text{-}\nu(C_6N_4)(5)$
Q22	1102.92	1102, 1116	1120	$\nu(N_4\text{-}N_3)(38)\text{-}\nu(CC)R1(22)+\beta(CH)R1(14)$
Q23	1056.39	1065		$\nu(CC)R2(49)\text{-}\beta(CH)R2(25)+ \tau R_{trz}(6)$
Q24	1017.15			$\delta_{TRI}R1(62)\text{-}\nu(C_{21}C_{22})R1(37)$
Q25	980.12			$\beta_{OUT}(CCH)R2(74)\text{-}\mu R_{trz}(6)$
Q26	858.88			β_{OUT} (CCH)R1(99)
Q27	728.44			$\tau R_{trz}(30)\text{-}\tau R1(10)\text{-}\delta_{ASYM}R1(7)+\beta_{OUT}(C_2C_6N_8)(6)+\delta_{ASYM}R2(5)+\beta_{OUT}(C_1C_2N_8)(5)$
Q28	719.27	726		$\tau R1(21)+ \tau R_{trz}(18)+\nu(C_2C_1)(6)$
Q29	678.13	676	670	$\tau R_{trz}(53)+ \beta_{OUT}(N_8C_6N_4)(34)$
Q30	630.47	646	615	$\delta_{ASYM}R2(46)\text{-}\delta_{ASYM}R1(21)\text{-}\tau_{ASYM}R2(15)$
Q31	552.67	564	564	$\beta_{OUT}(H_5C_6N_4)(63)\text{-}\tau R_{trz}(8)\text{-}\beta_{OUT}(N_4C_6S_7)(8)+\tau R1(6)+ \beta_{OUT}[C_2CC(R1)](5)$
Q32	482.52		470, 489	$\beta(C_9N_8)(11)\text{-}\beta_{OUT}[N_8CC(R2)](10)+\tau_{ASYM}R2(9)\text{-}\tau_{ASYM}R1(7)+\beta(C_2C_1)(6)\text{-}\beta(C_6S_7)(6)+\beta(C_2C_1)(6)\text{-}\beta_{OUT}(C_2N_8C_6)(5)\text{-}\beta_{OUT}(C_2CC(R1)(5)$
Q33	414.42		408	$\tau_{ASYM}R1(81)$
Q34	389.51		362	$\beta(C_9N_8)(24)\text{-}\tau_{ASYM}R2(14)+\tau_{ASYM}R1(12)+\beta(C_6S_7)(11)\text{-}\beta_{OUT}(C_2N_8C_9)(8)\text{-}\tau_{ASYM}R2(5)$
Q35	336.08		337	$\tau_{ASYM}R1(20)\text{-}\tau R_{trz}(17)+\beta_{OUT}(C_2C_1N_8)(16)+ \beta_{OUT}(C_6N_4N_3)(15)+ \beta(C_2C_1)(5)$
Q36	256.23		249	$\tau_{ASYM}R2(22)\text{-}\beta(C_2C_1)(10)\text{-}\beta(C_9N_8)(9)+\tau_{ASYM}R1(9)\text{-}\nu(C_2\text{-}N_8)(6)$

[a]Abbreviations; ν: stretching, μ: ring puckering, β: bending, δ: deformation, ρ: rocking, τ: torision, IN: in plane, OUT: out of plane, sym: symmetric, asym: asymmetric, LIN: linear bending. R1: benzene ring 1, R2: benzene ring 2, thd: thiadiazole ring, trz: triazole ring.

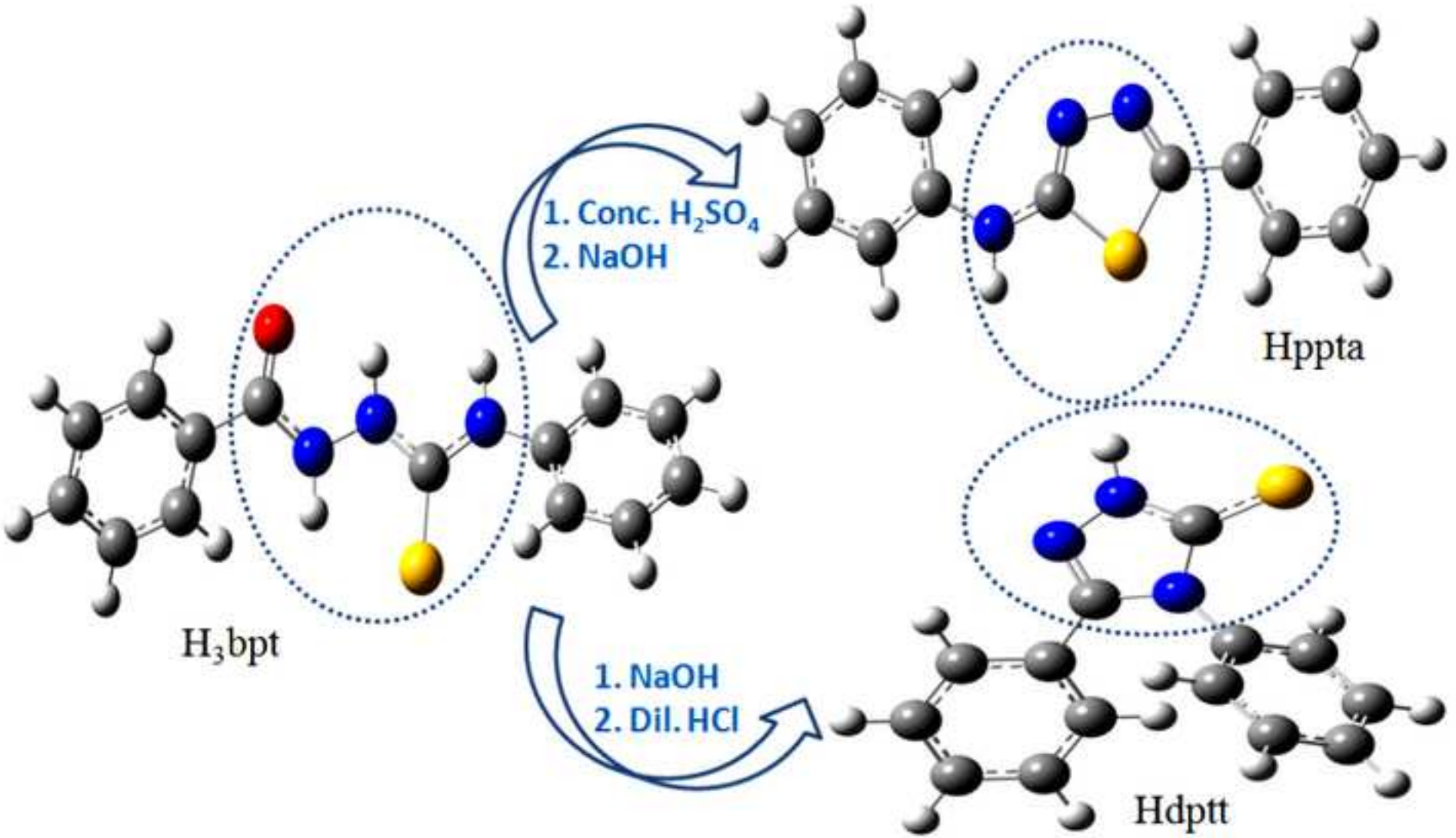
1. Conc. H_2SO_4
2. NaOH
Hppta
H_3bpt
1. NaOH
2. Dil. HCl
Hdptt

Highlights:

- 1-benzoyl-4-phenyl-3-thiosemicarbazide, N-phenyl-5-phenyl-1, 3, 4-thiadiazole-2-amine and 4, 5-diphenyl-2, 4-dihydro-1, 2, 4-triazole-3-thione have been synthesized.
- The cyclization of thiosemicarbazide group in 1-benzoyl-4-phenyl-3-thiosemicarbazide are investigated by using FT-IR, Raman and DFT method.
- The optimized geometries and MEPS plots performed by DFT method are reported.
- HOMO and LUMO have negative energies indicating the stability of synthesized compounds.